



Prognostic value of single-subject grey matter networks in early multiple sclerosis

Vinzenz Fleischer,^{1,†} Gabriel Gonzalez-Escamilla,^{1,†} Deborah Pareto,² Alex Rovira,² Jaume Sastre-Garriga,³ Piotr Sowa,⁴ Einar A. Høgestøl,^{5,6} Hanne F. Harbo,^{5,6} Barbara Bellenberg,⁷ Carsten Lukas,⁷ Serena Ruggieri,⁸ Claudio Gasperini,⁹ Tomas Uher,¹⁰ Manuela Vaneckova,¹¹ Stefan Bittner,¹ Ahmed E. Othman,¹² Sara Collorone,¹³ Ahmed T. Toosy,¹³ Sven G. Meuth,¹⁴ Frauke Zipp,¹ Frederik Barkhof,^{13,15} Olga Ciccarelli¹³ and Sergiu Groppa¹ on behalf of the MAGNIMS study group

[†]These authors contributed equally to this work.

The identification of prognostic markers in early multiple sclerosis (MS) is challenging and requires reliable measures that robustly predict future disease trajectories. Ideally, such measures should make inferences at the individual level to inform clinical decisions.

This study investigated the prognostic value of longitudinal structural networks to predict 5-year Expanded Disability Status Scale (EDSS) progression in patients with relapsing-remitting MS (RRMS). We hypothesized that network measures, derived from MRI, outperform conventional MRI measurements at identifying patients at risk of developing disability progression.

This longitudinal, multicentre study within the Magnetic Resonance Imaging in MS (MAGNIMS) network included 406 patients with RRMS (mean age = 35.7 ± 9.1 years) followed up for 5 years (mean follow-up = 5.0 ± 0.6 years). EDSS was determined to track disability accumulation. A group of 153 healthy subjects (mean age = 35.0 ± 10.1 years) with longitudinal MRI served as controls. All subjects underwent MRI at baseline and again 1 year after baseline. Grey matter atrophy over 1 year and white matter lesion load were determined. A single-subject brain network was reconstructed from T1-weighted scans based on grey matter atrophy measures derived from a statistical parameter mapping-based segmentation pipeline. Key topological measures, including network degree, global efficiency and transitivity, were calculated at single-subject level to quantify network properties related to EDSS progression. Areas under receiver operator characteristic (ROC) curves were constructed for grey matter atrophy and white matter lesion load, and the network measures and comparisons between ROC curves were conducted.

The applied network analyses differentiated patients with RRMS who experience EDSS progression over 5 years through lower values for network degree [$H(2) = 30.0$, $P < 0.001$] and global efficiency [$H(2) = 31.3$, $P < 0.001$] from healthy controls but also from patients without progression. For transitivity, the comparisons showed no difference between the groups [$H(2) = 1.5$, $P = 0.474$]. Most notably, changes in network degree and global efficiency were detected independent of disease activity in the first year. The described network reorganization in patients experiencing EDSS progression was evident in the absence of grey matter atrophy. Network degree and global efficiency measurements demonstrated superiority of network measures in the ROC analyses over grey matter atrophy and white matter lesion load in predicting EDSS worsening (all P -values < 0.05).

Our findings provide evidence that grey matter network reorganization over 1 year discloses relevant information about subsequent clinical worsening in RRMS. Early grey matter restructuring towards lower network efficiency predicts disability accumulation and outperforms conventional MRI predictors.

Received May 02, 2023. Revised July 17, 2023. Accepted August 02, 2023. Advance access publication August 29, 2023

© The Author(s) 2023. Published by Oxford University Press on behalf of the Guarantors of Brain.

This is an Open Access article distributed under the terms of the Creative Commons Attribution-NonCommercial License (<https://creativecommons.org/licenses/by-nc/4.0/>), which permits non-commercial re-use, distribution, and reproduction in any medium, provided the original work is properly cited. For commercial re-use, please contact journals.permissions@oup.com

- 1 Department of Neurology, Focus Program Translational Neuroscience (FTN) and Immunotherapy (FZI), Rhine Main Neuroscience Network (rmn2), University Medical Center of the Johannes Gutenberg University Mainz, 55131 Mainz, Germany
- 2 Section of Neuroradiology, Department of Radiology (IDI), Hospital Universitari Vall d'Hebron, Universitat Autònoma de Barcelona, 08035 Barcelona, Spain
- 3 Department of Neurology/Neuroimmunology, Multiple Sclerosis Centre of Catalonia, Hospital Universitari Vall d'Hebron, 08035 Barcelona, Spain
- 4 Division of Radiology and Nuclear Medicine, Oslo University Hospital, 0424 Oslo, Norway
- 5 Institute of Clinical Medicine, University of Oslo, NO-0316 Oslo, Norway
- 6 Department of Neurology, Oslo University Hospital, 0424 Oslo, Norway
- 7 Institute of Neuroradiology, St Josef Hospital, Ruhr-University Bochum, 44791 Bochum, Germany
- 8 Department of Neurosciences, Sapienza University of Rome, 00185 Rome, Italy
- 9 Department of Neurosciences, San Camillo-Forlanini Hospital, 00152 Rome, Italy
- 10 Department of Neurology and Center of Clinical Neuroscience, First Faculty of Medicine, Charles University and General University Hospital, 121 08 Prague, Czech Republic
- 11 Department of Radiology, First Faculty of Medicine, Charles University and General University Hospital, 121 08 Prague, Czech Republic
- 12 Department of Neuroradiology, University Medical Center of the Johannes Gutenberg University Mainz, 55131 Mainz, Germany
- 13 Department of Neuroinflammation, Queen Square MS Centre, UCL Queen Square Institute of Neurology, Faculty of Brain Science, University College of London, WC1E 6BT London, UK
- 14 Department of Neurology, Medical Faculty, Heinrich-Heine-University, 40225 Düsseldorf, Germany
- 15 Department of Radiology and Nuclear Medicine, Amsterdam UMC, 1100 DD Amsterdam, Netherlands

Correspondence to: Sergiu Groppa, MD, MBA

Department of Neurology, Focus Program Translational Neuroscience (FTN) and Immunotherapy (FZI), Rhine Main Neuroscience Network (rmn2), University Medical Center of the Johannes Gutenberg University Mainz, 55131 Mainz, Germany

E-mail: segroppa@uni-mainz.de

Keywords: relapsing-remitting multiple sclerosis; EDSS progression in MS; brain network measures; structural covariance; graph theory

Introduction

Multiple sclerosis (MS) is a chronic immune-mediated disease of the CNS characterized by inflammation, demyelination and neurodegeneration, which may lead to progressive disability.^{1–3} In particular, grey matter (GM) atrophy has been recognized as an important quantity related to disease progression,^{4,5} even at early disease stages.^{6,7} Even though GM atrophy detected by MRI is sensitive to the neurodegenerative component of MS, interindividual rates of atrophy vary.⁸

Recently, overall disability accumulation in relapsing-remitting MS (RRMS) was largely attributed to an underlying progressive disease course independent of relapse activity.^{9,10} Therefore, patients can show substantial heterogeneity in clinical progression rates over a longer period of time independent of relapse activity. This circumstance hampers the ability to detect patients with emerging disability within an early ‘window of opportunity’ for treatment optimization. Hence, biomarkers are needed that can help to distinguish individuals who will show rapid disability accumulation from those who will remain stable.

Atrophy measures alone do not take into account alterations in the topographic organization of the brain. One way to depict specific patterns of brain morphology is by representing them as a network.¹¹ In general, the two main MRI techniques that have been applied to investigate structural brain networks are 3D T1-weighted and diffusion tensor imaging.¹² Whereas the latter assesses white matter (WM) tissue microstructures, 3D T1-weighted scans provide anatomical imaging of WM and GM. In structural GM networks, connectivity

can be traced by assessing similarity in structural properties (e.g. cortical thickness or volume across subjects).¹³ The resultant covariance matrix can be described and quantified with graph theory.¹⁴ Here, nodes represent brain areas and the connections between nodes are termed edges when they have structural covariance. This analytical framework is proposed as being very sensitive to subtle structural alterations because microstructural damage to GM follows specific topographic patterns.^{11,13,15,16} Thus, structural covariance network analyses account for the spatial complexity of GM integrity at the entire brain level, have the advantage of being derived from anatomical MRI protocols and might be superior to conventional morphometric analyses for prediction of disease outcomes.^{14,17}

Network studies in MS based on interregional structural correlation analysis have demonstrated that brain circuits become disconnected and disintegrated, possibly to the extent of WM lesion load.¹⁸ Most studies have detected more segregated and less integrated structural networks at various MS stages.^{19–24} However, most of these studies addressed GM networks at group level, neglecting interindividual variability thus limiting their application to single-subject predictions of clinical courses.

The single-subject GM network analysis extends the group-level analysis by providing a reliable analytical framework of the individual GM morphology, and hence, a direct quantifiable link to behaviour or function.¹³ This approach facilitates the establishment of MRI-derived network properties as biomarkers in brain disorders. Recently, two cross-sectional studies applied this single-subject approach and demonstrated that a more random topology was related to cognitive dysfunction in both MS²⁴ and clinically isolated

syndrome (CIS).²⁵ This recent work suggests that the single-subject GM networks could contain crucial information explaining variance beyond conventional volumetric measures with promising potential for individual prediction of clinical courses.

In this study, we propose that structural GM networks may help to identify individual network properties critical for clinical deterioration in MS. Thus, the aim was to investigate the prognostic value of longitudinal GM networks using a single-subject approach in predicting the 5-year disability progression in MS as well as to contrast the network properties with the conventional atrophy measurements. To test this, we analysed individual GM networks from T1-weighted MRI scans within a large multicentre effort including 406 MS patients (followed up for 5 years to determine EDSS progression) and 153 healthy controls (HCs), both with longitudinal 3 T MRI at baseline and after 1 year.

Materials and methods

Patients and study design

This study was performed in accordance with good clinical practices and the Declaration of Helsinki. Approval was received from the local ethical committee. All participants gave written, informed consent for research within each centre prior to study participation. A Magnetic Resonance Imaging in Multiple Sclerosis (MAGNIMS) data-sharing agreement was signed among the participating centres.

For this multicentre, longitudinal, retrospective study, 406 patients with CIS and RRMS at seven European MAGNIMS centres with a disease duration of less than 5 years, who were relapse-free and received no corticosteroids for at least 30 days prior to enrollment were included between 2010 and 2021. Patients underwent both a clinical and an MRI evaluation at both the baseline and at the 1-year follow-up. In addition, all patients underwent a long-term clinical follow-up 5 years after baseline. Furthermore, we included 153 HCs without a history of neurological dysfunction who also had a follow-up MRI evaluation after 1 year. A graphical representation of the study timeline and design is shown in Fig. 1.

Clinical assessment

All patients underwent MRI and complete neurological evaluation at baseline, in which the Expanded Disability Status Scale (EDSS) score was determined and disease-modifying treatment (DMT) status was recorded. The first combined clinical and MRI follow-up assessment was performed in patients after a mean of 12.5 ± 4.4 months from study baseline. This follow-up included EDSS score assessments, recording of the DMT status and determining the presence and absence of disease activity in the first year using the composite score NEDA ('no evidence of disease activity') versus EDA ('evidence of disease activity') based on the established NEDA-3 criteria.²⁶ At the final clinical follow-up 5 years after baseline (5.0 ± 0.6 years), patients were clinically reassessed and EDSS progression was defined as an increase of ≥ 1 point in the EDSS score for a baseline score of ≥ 1.5 or a 1.5-point increase for a baseline score of 0.²⁷ Hence, we addressed accumulation of disability occurring in the early phase of the disease, but not conversion from the relapsing-remitting to the secondary progressive form of the disease.

Data acquisition

Structural MRI was performed longitudinally on in all seven participating centres [Barcelona and Mainz: Magnetom Trio (Siemens);

London and Bochum: Achieva (Philips); Oslo: Magnetom Avanto (Siemens); Prague: Magnetom Skyra (Siemens); Rome: Magnetom Avanto (Siemens)] without major changes to the hardware or the software during the follow-up investigation. The MRI acquisition protocol included the following sequences in all patients and HCs: high-resolution, isotropic, sagittal 3D T1-weighted sequence and sagittal 3D T2-weighted fluid-attenuated inversion recovery (FLAIR) sequence (Supplementary Table 1).

White matter lesion load estimation and lesion filling

White matter lesion load was automatically computed using the SPM12-based Lesion Segmentation Toolbox (LST).²⁸ 3D FLAIR images were co-registered to 3D T1-weighted images and bias corrected. After partial volume estimation, lesion segmentation was performed with 20 initial threshold values for the lesion growth algorithm. By comparing automatically and manually estimated lesion maps, the optimal threshold (κ value, dependent on image contrast) was determined for each patient and an average value for all patients was calculated.²⁸ Subsequently, a uniform κ value of 0.1 was applied in all patients for automatic lesion volume estimation and filling of 3D T1-weighted images. Then, the quality of the filled 3D T1-weighted images was visually inspected. Lesion-filled T1-weighted images were used for the computation based on regional GM properties.

Longitudinal MRI preprocessing

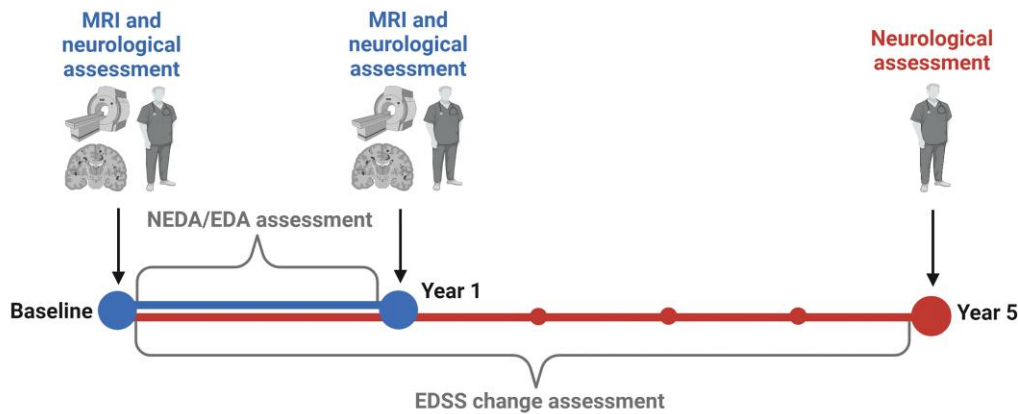
First, images were corrected for bias field inhomogeneity using the N4 algorithm.²⁹ For all pairs of T1-weighted anatomical MRI scans, a pairwise inverse-consistent alignment, as implemented in SPM12 software (<http://www.fil.ion.ucl.ac.uk/spm/>), was applied.³⁰ Initially, the first and second scans of each subject were aligned using a rigid-body transform. Then, non-linear pairwise alignment was performed by incorporating bias field correction. The resulting aligned images were averaged to obtain a within-subject mid-point image. The mid-point image was deformed to the first and second scans, resulting in Jacobian maps encoding the relative volume at each voxel between the scan and the mid-point average, from which the deformation velocities were computed and normalized by the time interval between the two scans (in years) and possible acquisition effects between the centres. Finally, the divergence of the initial velocities was computed to create a map of the divergence of the velocity field. In this map, negative values are considered the rate of volumetric contraction over 1 year.

Additionally, the mid-point registered images were segmented into GM, WM and CSF tissue compartments and normalized to MNI (Montreal Neurological Institute) space using DARTEL,³¹ a fast diffeomorphic image registration algorithm that minimizes anatomical variations among subjects while preserving topology.³² The segmentation was based on *a priori* tissue templates adapted to better delineate subcortical structures and to enhance the sensitivity of voxel-based morphometry, while being more optimal for younger populations than the standard ICBM (International Consortium of Brain Mapping) template.³³ The above-mentioned divergence map is entered into the single-subject GM network pipeline (see later and Fig. 2).

Single-subject grey matter networks

Following MRI preprocessing, the single-subject GM networks were reconstructed from GM tissue segmentations using an automated

Study timeline



Study design

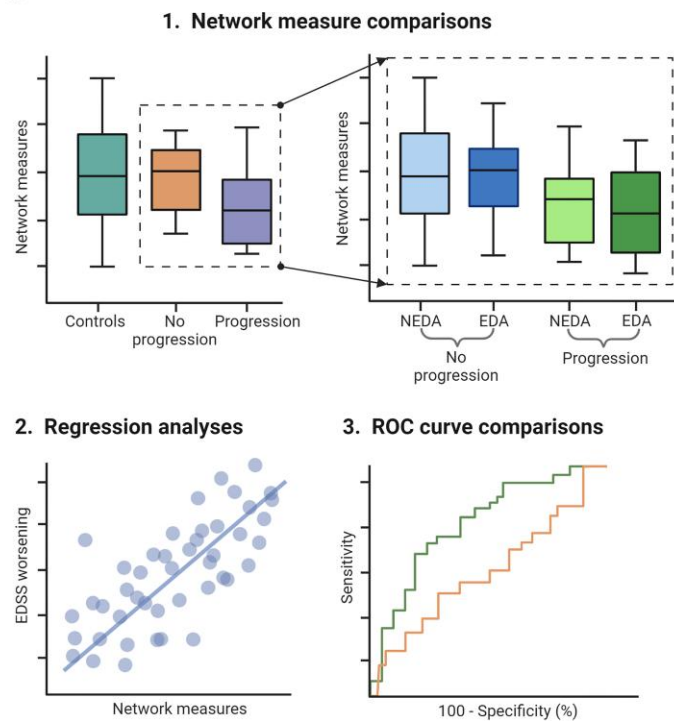


Figure 1 Study analysis design. Study timeline and design, including (1) network measure group comparisons; (2) regression analyses; and (3) receiver operating characteristic (ROC) curve comparisons. EDA = evidence of disease activity; EDSS = Expanded Disability Status Scale; NEDA = no evidence of disease activity.

method based on the generation of 3D cubes of a predefined size along the brain, which has been previously described in detail.¹³ This interregional covariance approach conceptualizes how morphological properties of different GM cubes relate to each other at the single-subject level and has been applied in MS populations before.^{24,25} In brief, network matrices were first constructed where the network nodes are defined as 6 mm³ voxel cubes and the network edges are defined by the GM covariance (i.e. Pearson's correlation) between the cube pairs. To account for the natural shape of the cortex, i.e. folding and curvature, and to identify the maximum correlation coefficient, the cubes are located at an angle to each other and rotated with multiples of 45°. By defining nodes as cubes, no *a priori* hypotheses about the regions of interest

need to be made, which is advantageous for whole brain connectivity analyses. Thus, both the folding structure of the cortex and the local GM information serve to assess the correlation between nodes.

To reduce the number of false positives, the constructed network matrices were binarized. The threshold was calculated as the proportion of connections that allow the network to be fully connected,¹³ avoiding the evaluation of fragmented networks. This ensures that group differences are not confounded by differing numbers of nodes and edges as for an absolute threshold at a single density.^{34,35}

Figure 2 shows a schematic overview of the applied approach, which is completely automated and data driven.

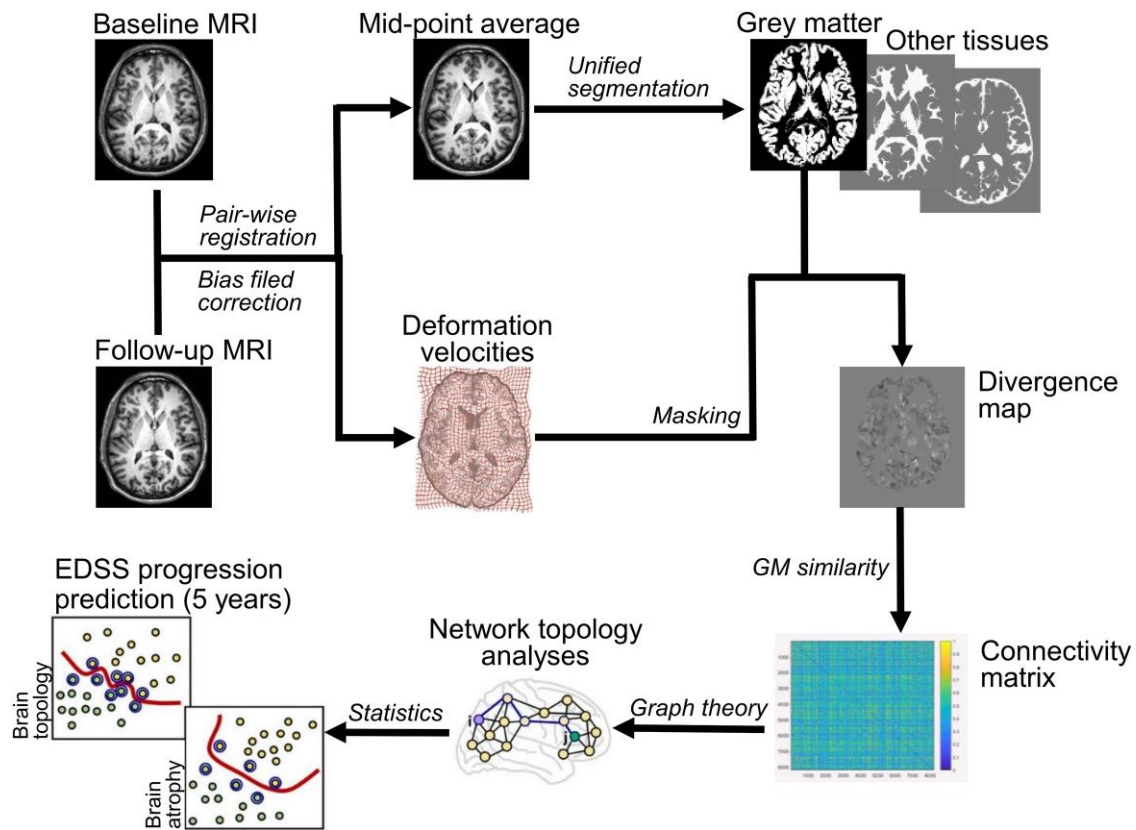


Figure 2 Methodological pipeline. General pipeline for the extraction of individual grey matter (GM) networks in a longitudinal setting. EDSS = Expanded Disability Status Scale.

Network properties measures

The network measures were calculated using functions from the Brain Connectivity Toolbox.³⁶ For each single-subject GM network, key network measures characterizing the essential topological architecture were computed: ‘network degree’ (centrality) to quantify the degree of connections in the network, ‘global efficiency’ as a network integration measure and ‘transitivity’ as a network segregation measure.

Network degree is the measure of centrality and quantifies the number or the degree of connections of the nodes in the network; thus, representing a measure of the extent to which a graph is connected.³⁶

Global efficiency is a network integration measure to describe information flow over the entire network.³⁶ It is the average of the shortest inverse path length between all of the nodes in the network.³⁷

The transitivity of the network is a measure of network segregation, reflecting the probability that two regions neighbour each other. Transitivity is based on the relative number of triangles in a graph compared with the total number of connected triples of regions.³⁸

Eventually, the resulting network measures represent the individual GM network dynamic change over 1 year.

Statistical analysis

The clinical and demographic data of patients and HCs were compared between groups using a Mann–Whitney U-test for continuous variables and Pearson’s chi-square test for categorical

variables (SPSS software, version 22.0; IBM). Unless otherwise indicated, data are expressed as mean ± standard deviation (SD).

For all network measures (network degree, global efficiency and transitivity) of the patients and the HCs, the Kolmogorov–Smirnov normality test was used to check whether data were distributed normally.

Network measures were compared between HCs, MS patients without EDSS progression and MS patients with EDSS progression. To determine whether 1-year changes in single-subject networks are related to current disease activity rather than to subsequent disability accumulation, we opted to divide MS patients into four groups based on their disease activity and their EDSS progression:

- (i) MS patients with NEDA in the first year and without EDSS progression (NP) over 5 years (NEDA+NP);
- (ii) MS patients with EDA in the first year, but without EDSS progression over 5 years (EDA+NP);
- (iii) MS patients with NEDA in the first year, but with EDSS progression (P) over 5 years (NEDA+P);
- (iv) MS patients with EDA in the first year and EDSS progression over 5 years (EDA+P).

To compare the network measures between groups, we performed the statistical inferences in a non-parametric Wilcoxon signed-ranks test (two groups) or Kruskal–Wallis test (greater than two groups), as most variables were not normally distributed. A *post hoc* Dunn–Bonferroni correction for multiple comparisons was applied to the significances obtained from the series of Kruskal–Wallis test results.

To test associations between network characteristics and clinical worsening over the 5-year period (EDSS worsening),

Table 1 Demographical, clinical and MRI data of MS patients and HCs at baseline and after division into MS patients with and without EDSS progression after 5 years of follow-up

	MS (n = 406)	HCs (n = 153)	NP (n = 291)	P (n = 115)	P-value (NP versus P)	P-value (MS versus HCs)
Sex, female/male	280/126	96/57	204/87	76/39	P = 0.431 ^a	P = 0.162 ^a
Mean (±SD) age at MRI, years	35.7 ± 9.1	35.0 ± 10.1	35.3 ± 8.9	36.9 ± 9.5	P = 0.114 ^b	P = 0.142 ^b
Mean (±SD) MRI follow-up, months	12.5 ± 4.4	12.0 ± 1.2	12.6 ± 4.3	12.3 ± 4.6	P = 0.424 ^b	P = 0.563 ^b
Mean (±SD) clinical follow-up, years	5.0 ± 0.6	–	5.0 ± 0.6	5.0 ± 0.6	P = 0.695 ^b	–
Mean (±SD) age at onset, years	32.8 ± 9.1	–	32.3 ± 8.9	34.1 ± 9.7	P = 0.090 ^b	–
Mean (±SD) disease duration, years	2.7 ± 3.3	–	2.6 ± 3.2	3.2 ± 3.5	P = 0.103 ^b	–
Median (range) EDSS at baseline	1.5 (0–6.5)	–	1.5 (0–6.5)	1.5 (0–5.5)	P = 0.788 ^b	–
Disease course at baseline, CIS/RRMS	115/291	–	87/204	28/87	P = 0.264 ^a	–
NEDA/EDA first year	219/187	–	174/117	45/70	P < 0.001 ^a	–
EDSS progression over 5 years, no/yes	291/115	–	–	–	–	–
DMT at baseline, no/moderate ^c /high ^d	132/210/64	–	94/151/46	38/59/18	P = 0.990 ^a	–
Mean WM LL at baseline, ml	3.5 ± 4.3	–	3.5 ± 4.3	3.7 ± 4.1	P = 0.904 ^b	–
Mean GMV at baseline, ml	620.8 ± 67.0	656.6 ± 61.1	623.3 ± 67.1	614.0 ± 66.7	P = 0.224 ^b	P < 0.001 ^b

CIS = clinically isolated syndrome; DMT = disease-modifying treatment; EDA = evidence of disease activity; EDSS = Expanded Disability Status Scale; GMV = grey matter volume; HCs = healthy controls; MS = multiple sclerosis; NEDA = no evidence of disease activity; NP = no (EDSS) progression; P = (EDSS) progression; RRMS = relapsing-remitting multiple sclerosis; SD = standard deviation; WM LL = white matter lesion load.

^aP-value derived from Pearson's chi-square test (sex, disease course, NEDA/EDA and DMT).

^bP-value derived from Mann-Whitney U-test (age at MRI, follow-up time, age at onset, disease duration, EDSS, WM LL and GMV).

^cModerate efficiency DMT = glatiramer acetate, interferon-beta, teriflunomide, dimethyl fumarate, azathioprine.

^dHigh efficiency DMT = fingolimod, natalizumab, rituximab, mitoxantrone.

we performed linear regression analyses, including age, sex, disease duration, the initial EDSS status and the DMT status as covariates in the model.

Finally, receiver operating characteristic (ROC) curve analyses were conducted to examine the predictive power of network measures that discriminate patients with and without EDSS progression. Thus, ROC curves were calculated to determine the area under the curve (AUC) using MedCalc software (version 20.211). Only those network measures that were significantly different in the prior group comparisons were selected.

In a first step, the AUC for the network measures, as well as for GM atrophy and WM lesion load, were constructed, and the resulting sensitivities were plotted against the corresponding false positive rates. The AUCs with 95% confidence intervals (CIs) and P-values for testing AUC = 0.5 versus AUC ≠ 0.5 were calculated.

In a second step, we also compared the AUCs among each other to test for statistical significance of the difference between the curves.³⁹ P-values less than 0.05 were considered statistically significant.

Results

Demographic and clinical assessment

The demographic, clinical and MRI data from the HCs and MS patients are summarized in [Table 1](#), in combination and after division into MS patients with and without EDSS progression.

In total, 406 MS patients (280 female; mean age 35.7 ± 9.1 years) and 153 HCs (96 female; mean age 35.0 ± 10.1 years) were followed-up with MRI after 1 year with a mean follow-up of 12.5 ± 4.4 and 12.0 ± 1.2 months, respectively (P = 0.563). MS patients were followed-up for clinical (EDSS) reassessment after 5 years (5.0 ± 0.6 years) and the follow-up time did not differ between patients with (5.0 ± 0.6 years) and without EDSS progression (5.0 ± 0.6 years) (P = 0.695). Of the 406 MS patients, 115 (28.3%) had EDSS worsening over the clinical follow-up time, while 291 (71.7%) had no progression. Patients with and

without EDSS progression differed in their disease activity in the first year (P < 0.001) but not in the remaining comparisons ([Table 1](#)).

Grey matter atrophy over 1 year and white matter lesion load

Over the 1-year MRI follow-up, GM atrophy was not significant between HCs and all MS patients (Z = -1.9, P = 0.055; [Supplementary Fig. 1B](#)). However, there were significant groupwise effects for the comparison between HCs and MS patients with and without EDSS progression [H(2) = 6.4, P = 0.041; [Fig. 3B](#)]. Post hoc analyses revealed a significant difference between HCs and MS patients with EDSS progression (P = 0.035) only, after adjustment for multiple comparisons. No other comparisons were significant. The comparison of GM atrophy after subdivision into the four groups based on NEDA/EDA and EDSS progression showed no differences between the groups [H(3) = 6.0, P = 0.110; [Fig. 4B](#)].

Finally, the WM lesion load at baseline did not differ between MS patients with and without EDSS progression (Z = -1.2, P = 0.904), and it also did not differ between the four MS groups (NEDA/EDA each with and without EDSS progression) [H(3) = 2.9, P = 0.413].

Classifying grey matter network changes over 1 year based on subsequent EDSS progression status

The Wilcoxon signed-ranks test indicated that network degree was significantly lower in MS patients compared with HCs (Z = -2.3, P = 0.022; [Supplementary Fig. 1A](#)). After dividing the MS group into patients with and without EDSS progression over 5 years, there was a significant effect for network degree between the three groups [H(2) = 30.0, P < 0.001; [Fig. 3A](#)]. Post hoc tests revealed a significant difference between MS patients with and without EDSS progression (P < 0.001) and between HCs and MS patients with EDSS progression (P < 0.001), each with lower values in patients with subsequent progression. There was no difference between HCs and MS patients without EDSS progression (P = 1.0). The lower values of network

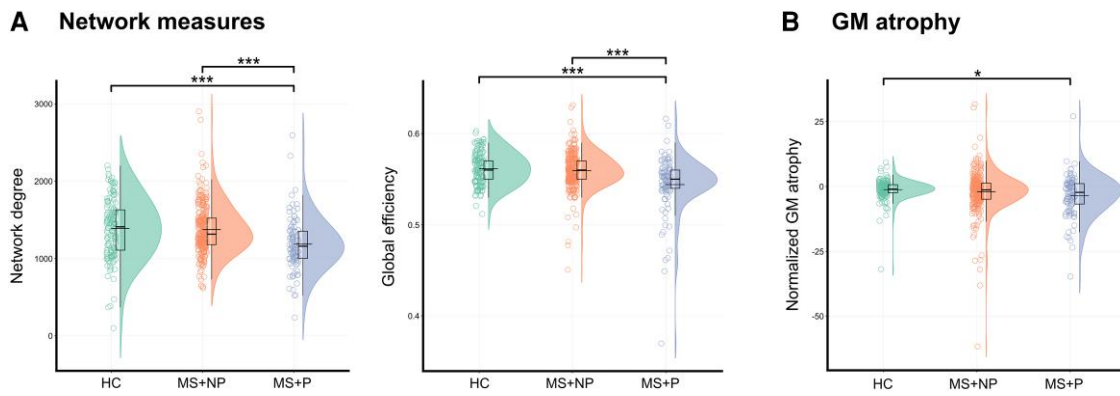


Figure 3 Network measures between healthy controls and multiple sclerosis patients with (P) and without (NP) Expanded Disability Status Scale (EDSS) progression over 5 years. The plots show the mean and standard deviation values of (A) network degree and global efficiency and (B) grey matter (GM) atrophy. * $P < 0.05$, ** $P < 0.001$, *** $P < 0.0001$. HC = healthy controls; MS+NP = multiple sclerosis patients without EDSS progression; MS+P = multiple sclerosis patients with EDSS progression.

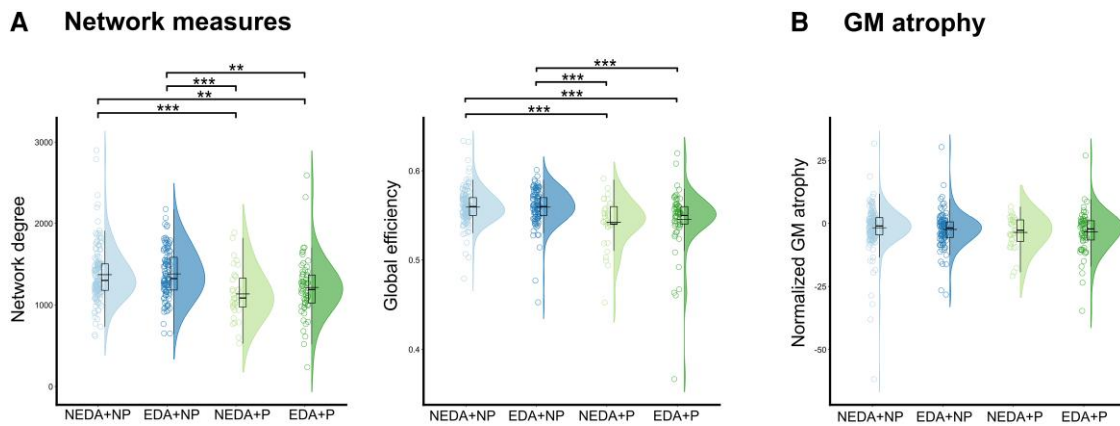


Figure 4 Network measures between multiple sclerosis (MS) patients with (P) and without (NP) Expanded Disability Status Scale (EDSS) progression over 5 years, depending on their disease activity in the first year. The plots show the mean and standard deviation values of (A) network degree and global efficiency and (B) grey matter (GM) atrophy. * $P < 0.05$, ** $P < 0.001$, *** $P < 0.0001$. Disease activity was defined by the ‘no evidence of disease activity’ concept (NEDA) versus ‘evidence of disease activity’ (EDA). NEDA+NP = MS patients with NEDA in the first year and without EDSS progression over 5 years; EDA+NP = MS patients with EDA in the first year, but without EDSS progression over 5 years; NEDA+P = MS patients with NEDA in the first year, but with EDSS progression over 5 years; EDA+P = MS patients with EDA in the first year and EDSS progression over 5 years.

degree in MS patients with EDSS progression indicate a generally less connected network.

Global efficiency was lower in MS patients compared with HCs ($Z = -2.3$, $P = 0.022$; [Supplementary Fig. 1A](#)). In the three-group comparison, there was a significant effect between the groups [$H(2) = 31.3$, $P < 0.001$; [Fig. 3A](#)]. Post hoc tests demonstrated a significant difference between MS patients with and without EDSS progression ($P < 0.001$) and between HCs and MS patients with EDSS progression ($P < 0.001$). Lower values were observed in patients with subsequent progression over 5 years. The post hoc comparison between HCs and MS patients without EDSS progression was not significant ($P = 1.0$). This global efficiency decrease in patients with EDSS progression suggests GM reorganization towards a structure with less long-range connections.

For the network measure transitivity, the initial comparison between all MS patients and HCs showed no significant difference ($Z = -0.001$, $P = 0.999$). Likewise, the comparison between HCs and MS patients with and without EDSS progression also showed no significant difference in transitivity between the three groups [$H(2) = 1.5$, $P = 0.474$]. Stable transitivity measures in all subjects indicate a maintained homogenization of neighbouring regions.

Grey matter network changes over 1 year based on NEDA/EDA status and subsequent EDSS progression

To determine whether 1-year changes in single-subject networks are related to current disease activity rather than to subsequent disability accumulation, we opted to divide MS patients into four groups based on their disease activity and their EDSS progression (see the ‘Materials and methods’ section).

The comparison between the four subdivided groups showed that the effect of group significantly influenced all network measures ([Fig. 4](#)).

There were significant differences between the four groups for the network degree measurements [$H(3) = 29.2$, $P < 0.001$; [Fig. 4A](#)]. Post hoc tests were performed and showed lower values for NEDA+P compared with NEDA+NP ($P < 0.001$) and EDA+NP ($P < 0.001$). Furthermore, EDA+P showed lower values compared with NEDA+NP ($P = 0.005$) and EDA+NP ($P = 0.002$). None of the other comparisons were significant after adjustment.

For global efficiency, there was a significant effect between the four groups [$H(3) = 30.4$, $P < 0.001$; [Fig. 4A](#)]. Post hoc tests revealed lower global efficiency values for NEDA+P compared with

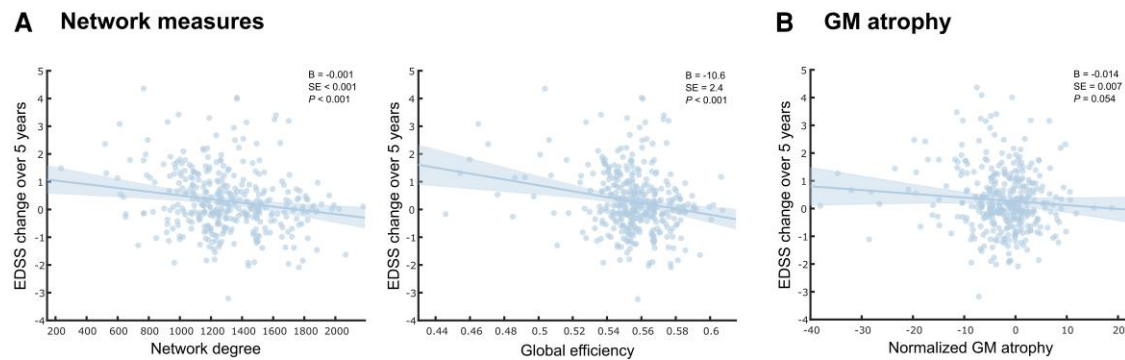


Figure 5 Association of Expanded Disability Status Scale (EDSS) change over 5 years with network measures and grey matter atrophy over 1 year. EDSS change over 5 years in relation to (A) the respective network measures (network degree and global efficiency) and (B) grey matter (GM) atrophy by multiple linear regressions adjusted for age, sex, disease duration, the initial EDSS status and the disease-modifying treatment status.

ROC curves

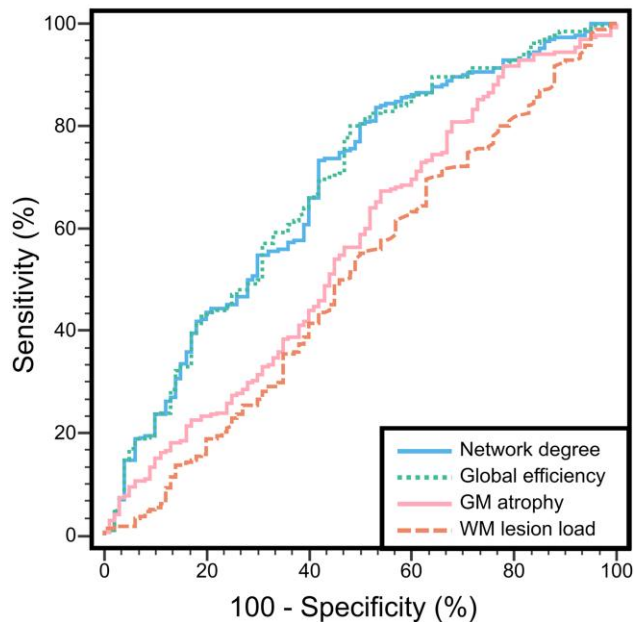


Figure 6 Receiver operating characteristic (ROC) curves with areas under the curve. ROC curves of network degree and global efficiency as well as grey matter (GM) atrophy and white matter (WM) lesion load, discriminating multiple sclerosis patients with subsequent Expanded Disability Status Scale (EDSS) progression from those without EDSS progression over 5 years.

NEDA+NP ($P < 0.001$) and EDA+NP ($P < 0.001$). In addition, EDA+P showed lower values compared with NEDA+NP ($P = 0.005$) and EDA+NP ($P = 0.001$). No other comparisons were significant after adjustment for multiple comparisons.

For transitivity, our results demonstrated no significant differences between the four groups [$H(3) = 3.0$, $P = 0.386$].

Association of grey matter network changes over 1 year with EDSS changes over 5 years

EDSS worsening over 5 years was then related to the respective longitudinal network measures over 1 year (network degree, global efficiency and transitivity) by multiple linear regressions and adjusted for age, sex, disease duration, the initial EDSS status and

the DMT status. Higher (more positive) values in EDSS changes indicated greater disability accumulation over 5 years. EDSS worsening over 5 years was associated with both lower network degree [$B = -0.001$, standard error (SE) < 0.001 , $P < 0.001$; Fig. 5A] and lower global efficiency ($B = -10.6$, SE = 2.4, $P < 0.001$; Fig. 5A). EDSS worsening was not significantly associated with transitivity ($B = 2.7$, SE = 3.1, $P = 0.370$).

Discriminative power of longitudinal grey matter networks over 1 year in predicting EDSS progression

Finally, an overall ROC analysis was performed to determine the predictive discriminating value of longitudinally acquired network measures to distinguish MS patients with and without EDSS progression over 5 years. Resulting values with AUC, standard error, 95% CI and P-values are presented in detail in Fig. 6. In summary, for network degree (AUC = 0.677, 95% CI = 0.626–0.724) and global efficiency (AUC = 0.680, 95% CI = 0.629–0.727), the P-values for testing AUC = 0.5 versus AUC \neq 0.5 were less than 0.001. In contrast, GM atrophy (AUC = 0.557, 95% CI = 0.505–0.608) and WM lesion load (AUC = 0.504, 95% CI = 0.454–0.554) were not significantly different from a random classifier ($P > 0.05$), meaning both markers have no class separation capacity (Table 2).

In a last step, a comparison of ROC curves was conducted to test the statistical significance of the difference between the areas under the four ROC curves (network degree, global efficiency, GM atrophy and WM lesion load). This analysis of differences between AUCs demonstrated that the AUC of the ROC curve from network degree was significantly larger than the AUCs from GM atrophy (Δ AUC = 0.117, 95% CI = 0.024–0.211, $P = 0.014$) and WM lesion load (Δ AUC = 0.173, 95% CI = 0.081–0.265, $P < 0.001$). In addition, the AUC of the ROC curve from global efficiency was significantly larger than the AUCs from GM atrophy (Δ AUC = 0.120, 95% CI = 0.027–0.214, $P = 0.012$) and WM lesion load (Δ AUC = 0.176, 95% CI = 0.083–0.268, $P < 0.001$). These results indicate superiority of network degree and global efficiency over GM atrophy and WM lesion load in discriminating MS patients with and without EDSS progression (Table 2).

Discussion

Our study provides evidence for structural network alterations in early MS patients experiencing EDSS progression after 5 years. Here, single-subject brain networks were reconstructed from

Table 2 ROC curve results and comparisons

	AUC	SE	95% CI	P-value
ROC				
Network degree	0.677	0.032	0.626–0.724	<0.001
Global efficiency	0.680	0.032	0.629–0.727	<0.001
GM atrophy	0.557	0.035	0.505–0.608	0.103
WM lesion load	0.504	0.034	0.454–0.554	0.907
ROC comparisons				
Network degree versus GM atrophy	0.117	0.048	0.024–0.211	0.014
Network degree versus WM lesion load	0.173	0.047	0.081–0.265	<0.001
Global efficiency versus GM atrophy	0.120	0.048	0.027–0.214	0.012
Global efficiency versus WM lesion load	0.176	0.047	0.083–0.268	<0.001
Network degree versus Global efficiency	0.003	0.003	–0.004–0.010	0.413
GM atrophy versus WM lesion load	0.055	0.053	–0.048–0.158	0.293

Receiver operating characteristic (ROC) curve results and comparisons of ROC curves to assess superiority of one of these measures over the others.

Bold values denote statistical significance at the $P < 0.05$ level.

AUC = area under the curve; CI = confidence interval; GM = grey matter; SE = standard error; WM = white matter.

longitudinal T1-weighted MRI scans based on 1-year GM atrophy measures and network properties were determined and related to EDSS progression. We identified a decline in key network properties shown by reduced network degree and global efficiency in MS patients with subsequent EDSS progression compared with non-progressive MS patients and most notably, this was independent of disease activity in the first year. The observed network reorganization was evident beyond detectable atrophy as characterized by conventional methods. Lastly, the individual GM network measures even outperformed conventional MRI measurements in identifying MS patients at risk for disability accumulation. All calculated network measures, as well as classical GM atrophy, consistently showed no difference between controls and MS patients without 5-year EDSS progression. This supports the premise that GM pathology over 1 year in non-progressive MS patients may not be sensitive enough to be detected. Strikingly, network measures were significantly different between patients with and without EDSS progression, in spite of no significant differences in GM atrophy between them. Thus, our findings show that network degree and global efficiency derived from individual GM network analyses capture additional information beyond simple GM volumetry and that this hidden information is clinically relevant.

In our predictive modelling approach, we complemented this observation by demonstrating a significant superiority of both network measures (network degree and global efficiency) over conventional MRI measures (GM atrophy and WM lesion load) in discriminating patients with EDSS progression from those without progression. Moreover, we aimed to elucidate whether the presence or absence of disease activity over 1 year influences the network measures between patients with and without subsequent EDSS progression over the following 5 years. Earlier work has demonstrated that disease activity using the NEDA composite score over 1 year likely does not influence GM network measures using a conventional group-level approach.¹⁹ This suggests that both

active and stable MS patients show similar alterations within the cortex which is captured by structural covariance networks. Our single-subject approach confirmed that NEDA status over 1 year does not associate with network measures over 1 year. However, subsequent disability accumulation seems to be dependent upon early differences in network measures, as also recently shown for MS-related fatigue in a large multicentre study.⁷ Moreover, a longitudinal network study demonstrated reorganizational changes towards a disrupted GM network in CIS patients, highlighting the clinical relevance of early GM network changes.²⁰

Here, MS patients without EDSS progression exhibited a stable GM network (compared with HCs) irrespective of their first-year disease activity. In comparison, MS patients with EDSS progression demonstrated GM network alterations, again independent of their first-year disease activity status. Taken together, the evidence of network reorganization based on EDSS progression and not based on disease activity supports the view that early GM restructuring occurs regardless of observable disease activity.¹⁹

Our findings provide the brain network equivalent to accumulating evidence from neuropathological,⁴⁰ conventional imaging⁴¹ and recent clinical⁹ studies suggesting a more insidious structural damage in MS across all phenotypes. This considers MS as a disease continuum with relapse-associated worsening, but also with progression independent of relapse activity early in the disease.^{10,42} It is biologically plausible that this early progressive and neurodegenerative continuum of the disease is reflected by a loss of GM integrity and thus by alterations in structural GM networks. Against this background, the individual GM networks, as shown by our findings, might serve as an advanced imaging criterion to mark upcoming disability accumulation in early MS. This would be particularly advantageous because the detection of EDSS progression in MS patients with a relapse onset and generally mild disability is challenging due to the inherent lack of granularity and reproducibility of clinical metrics.⁹

Our results depict GM reorganization preceding beyond the established measures of GM atrophy. The GM network architecture is more randomly constructed in those MS patients experiencing disability accumulation compared to MS patients without EDSS worsening. Decreased global efficiency indicating impaired integration represents a less efficient network organization principle of biological systems.^{14,43} This network imbalance between impaired integration and preserved segregation (unchanged transitivity) might depict either direct cortical GM damage or an early maladaptive response of the cortex in order to deal with chronic inflammation, of which both can explain the observed clinical deterioration.

In a recent individual GM network approach in a cross-sectional setting, a more random network organization was related to inter individual worsening in cognitive function in MS.²⁴ In line with this, CIS patients showed altered network properties in several cortical regions, including areas relevant to cognition.²⁵ At group level, an early study showed that an increased WM lesion load in MS is associated with a decrement in cortical network efficiency,¹⁸ substantiating the hypothesis that WM lesions lead to axonal transection and subsequent retrograde degeneration, contributing eventually to cortical atrophy.⁴⁴ In our study, WM lesion load did not differ between patients with and without EDSS progression. This observation fits the assumption that GM integrity loss in MS may be partly independent of axonal transection (through lesions) and that there is an additional primary neurodegenerative process related to other disease mechanisms, perhaps including meningeal inflammation.⁴⁵

Recently, the WM network properties on MRI were found to be associated with neuronal size and axonal density in a post-mortem *in situ* whole-brain diffusion tensor imaging study, indicating that macro-scale network measures may reveal neuroaxonal degeneration in MS.⁴⁶ Considering that WM- and GM-derived networks exhibit a similar network organization in MS patients,^{22,47} our data suggest that early EDSS progression seems to originate from a microstructurally disintegrated network which may precede MRI-detectable GM atrophy later on. Hence, individual GM networks derived from generally available MRI sequences could provide sensitive and robust biomarkers aimed at detecting MS patients experiencing disability accumulation.

One possible limitation of our study stems from our unique design of combining 1-year MRI and 5-year clinical follow-up data, whereby possible later network changes (between Years 2 and 5) are not captured by nature. However, structural networks in MS change early in the disease and already in short-time intervals.^{20,47} Hence, the 1-year MRI follow-up in our large cohort is less prone to potential fluctuations that might come up over a 5-year period. In addition, a biomarker obtained over 5 years in order to predict clinical worsening is clinically less meaningful. Another consideration refers to the fact that study baseline was not necessarily at disease onset in all patients. However, all included patients had a disease duration of less than 5 years at baseline and, thus, were clearly in the early phase of the disease. This, in turn, limits the generalizability of our results to other types of MS. Moreover, the EDSS score as our outcome measure is limited by its poor assessment of upper limb function, fatigue and cognitive impairment. However, despite its disadvantages, it is still the most established score for evaluating MS progression in clinical trials and routine clinical practice. In this regard, it is worth noting that EDSS progression was not confirmed after the 5-year follow-up, which might have provided a more accurate evaluation of irreversible disability accrual.²⁷ Furthermore, we did not include a spinal cord MRI evaluation, which may be relevant for disability accumulation besides brain damage.⁴⁸

Future studies should evaluate the impact of longitudinal network properties on other clinical outcomes, such as cognitive performance and patients' reported outcomes. Recent evidence endorses the existence of network changes in radiologically isolated syndrome suggesting that network alterations can even start years before clinical manifestations.⁴⁹ There are also the questions of whether and how the network changes in MS patients with relapse onset before transitioning to the progressive form. Current evidence suggests that the network might 'collapse' after passing a critical threshold of efficiency loss.^{14,43} In addition, several attempts have highlighted a convergence of GM covariance networks with diffusion MRI connections⁵⁰ as well as functional connectivity⁵¹ suggesting that GM networks also contain information about correlated intrinsic functional activity and potentially cellular mechanisms behind structural covariance, e.g. synaptic physiology.⁵² Thus, the integration of both structural and functional network MRI measures may aid the identification of specific circuits critical for clinical deterioration.⁵³

In conclusion, our findings demonstrate that GM network alterations over 1 year predict subsequent clinical worsening in MS. The individual GM networks are sensitive to an underlying progressive disease course and largely independent of relapse activity. Early GM restructuring towards a less efficient network precedes EDSS progression and outperforms conventional MRI predictors. Hence, longitudinal single-subject networks provide promising MRI-based markers to track disability accumulation in MS.

Data availability

Data availability is subject to specific agreements between the Department of Neurology of the University Medical Center Mainz and each participating MAGNIMS centre. Both the MRI and the processed data are available upon reasonable request from a qualified investigator and data transfer approval with the corresponding centre.

Acknowledgements

The authors thank all the patients who participated in the study. We thank Cheryl Ernest and Kathleen Claussen for proof-reading. The illustrations were adapted from BioRender.com templates and retrieved from <https://app.biorender.com/biorender-templates>.

Funding

This work was supported by a grant from the German Research Council (Deutsche Forschungsgemeinschaft (D.F.G.); CRC-TR-128; V.F., S.B., F.Z., S.G.), by the National MS Society USA, grant RFA-220339314 (S.G.), by the DFG (Radiomics SPP 2177, S.G., G.E.G.), grants GR 4590/3-1 and GO 3493/1-1, by the German Federal Ministry for Education and Research, BMBF, German Competence Network Multiple Sclerosis (KKNMS), grants 01GI1601I and 01GI0914, and by the 'Oppenheim-Förderpreis für Multiple Sklerose' of Novartis Pharma GmbH (V.F.). In addition by the Research Council of Norway (Grant No. 240102, PI: H.F.H.), by the South-Eastern Regional Health Authorities of Norway (Grant No. 2011059 and ES563338/Biotek 2021, PI: H.F.H.) and by the Instituto de Salud Carlos III PI18/00823 (D.P.). The contribution of data from Prague (T.U. and M.V.) was supported by the Ministry of Health of the Czech Republic within the conceptual development of a research organization (00064165) at the General University Hospital in Prague, by the project National Institute for Neurological Research and by the European Union—Next Generation EU (Programme EXCELES, ID project No LX22NPO5107) and by Roche (NCT03706118).

Competing interests

V.F. received research support from Novartis. D.P. has received a research contract from Biogen Idec and receives research support from Fondo de Investigación en Salud (PI18/00823) from Instituto de Salud Carlos III, Spain. A.R. serves on scientific advisory boards for Novartis, Sanofi-Genzyme, Synthetic MR, TensorMedical, Roche, Biogen and OLEA Medical and has received speaker honoraria from Bayer, Sanofi-Genzyme, Merck-Serono, Teva Pharmaceutical Industries Ltd., Novartis, Roche, Bristol-Myers and Biogen. J.S.G. declares fees from Sanofi, Biogen, Celgene, Merck, Biopass, Novartis and Roche and receives research support from Fondo de Investigación en Salud (PI19/00950) from Instituto de Salud Carlos III, Spain. P.S. has received honoraria for lecturing and travel support from Merck. E.A.H. received honoraria for lecturing and advisory board activity from Biogen, Merck and Sanofi-Genzyme and an unrestricted research grant from Merck. H.F.H. has received travel support, honoraria for advice or lecturing from Biogen Idec, Sanofi-Genzyme, Merck, Novartis, Roche and Teva and an unrestricted research grant from Novartis. B.B. received financial support from the German Federal Ministry for

Education and Research, BMBF, German Competence Network Multiple Sclerosis (KKNMS), Grant No. 01GI1601I. C.L. received a research grant from the German Federal Ministry for Education and Research, BMBF, German Competence Network Multiple Sclerosis (KKNMS), Grant No. 01GI1601I, and has received consulting and speaker's honoraria from Biogen Idec, Bayer Schering, Daiichi Sanykyo, Merck Serono, Novartis, Sanofi, Genzyme and Teva. S.R. has received honoraria from Biogen, Merck Serono, Novartis and BMS for consulting services, speaking and/or travel support. C.G. has received speaker honoraria and/or travel expenses for attending meeting from Bayer Schering Pharma, Sanofi-Aventis, Merck, Biogen, Novartis and Almirall. T.U. has received financial support for conference travel and honoraria from Biogen Idec, Novartis, Roche, Genzyme and Merck Serono, as well as support for research activities from Biogen Idec and Sanofi. M.V. received speaker honoraria and consultant fees from Biogen Idec, Novartis, Sanofi Genzyme, Roche and Teva, as well as support for research activities from Biogen Idec and institutional support from the Czech Ministry of Health (RVO-VFN 64165) and Education (Cooperatio LF1, research area Neuroscience). S.B. has received honoraria and compensation for travel from Biogen Idec, Merck Serono, Novartis, Sanofi-Genzyme and Roche. S.C. is supported by the Rosetrees Trust (MS632), and she was awarded a MAGNIMS-ECTRIMS fellowship in 2016. A.T.T. has received speaker honoraria from Biomedica, Sereno Symposia International Foundation and Bayer, and meeting expenses from Biogen Idec, and is the UK PI for two clinical trials sponsored by MedDay Pharmaceuticals. S.G.M. received honoraria for lecturing and travel expenses for attending meetings from Almirall, Amicus Therapeutics Germany, Bayer Health Care, Biogen, Bristol Myers Squibb/Celgene, Diamed, Genzyme, MedDay Pharmaceuticals, Merck Serono, Novartis, Novo Nordisk, Ono Pharma, Roche, Sanofi-Aventis, Chugai Pharma, QuintilesIMS and Teva. His research is funded by the German Ministry for Education and Research, Bundesinstitut für Risikobewertung, Deutsche Forschungsgemeinschaft, Else Kröner Fresenius Foundation, Gemeinsamer Bundesausschuss, German Academic Exchange Service, Hertie Foundation, Interdisciplinary Center for Clinical Research Muenster, German Foundation Neurology, Alexion, Almirall, Amicus Therapeutics Germany, Biogen, Diamed, Fresenius Medical Care, Genzyme, HERZ Burgdorf, Merck Serono, Novartis, Ono Pharma, Roche and Teva. F.Z. has recently received research grants and/or consultation funds from DFG, BMBF, PMSA, MPG, Genzyme, Merck Serono, Roche, Novartis, Sanofi-Aventis, Celgene, ONO and Octapharma. F.B. is supported by the NIHR Biomedical Research Centre initiative at UCLH, serves on the editorial boards of *Brain*, *European Radiology*, *Journal of Neurology*, *Neurosurgery & Psychiatry*, *Neurology*, *Multiple Sclerosis*, and *Neuroradiology*, and serves as consultant for Bayer Schering Pharma, Sanofi-Aventis, Biogen-Idec, Teva Pharmaceuticals, Genzyme, Merck-Serono, Novartis, Roche, Synthon, Jansen Research and Lundbeck. O.C. receives research grant support from the Multiple Sclerosis Society of Great Britain and Northern Ireland, the NIHR and the NIHR UCLH Biomedical Research Centre. She is the Deputy Editor of *Neurology*, for which she receives an honorarium, and she has received honoraria from Novartis and Biogen. The other authors report no competing interests.

Supplementary material

Supplementary material is available at *Brain* online.

References

- Filippi M, Bruck W, Chard D, et al. Association between pathological and MRI findings in multiple sclerosis. *Lancet Neurol*. 2019;18:198-210.
- Attfeld KE, Jensen LT, Kaufmann M, Friese MA, Fugger L. The immunology of multiple sclerosis. *Nat Rev Immunol*. 2022;22:734-750.
- Groppa S, Gonzalez-Escamilla G, Eshaghi A, Meuth SG, Ciccarelli O. Linking immune-mediated damage to neurodegeneration in multiple sclerosis: Could network-based MRI help? *Brain Commun*. 2021;3:fcab237.
- Filippi M, Preziosa P, Rocca MA. Magnetic resonance outcome measures in multiple sclerosis trials: time to rethink? *Curr Opin Neurol*. 2014;27:290-299.
- Muthuraman M, Fleischer V, Kroth J, et al. Covarying patterns of white matter lesions and cortical atrophy predict progression in early MS. *Neurol Neuroimmunol Neuroinflamm*. 2020;7:e681.
- Eshaghi A, Marinescu RV, Young AL, et al. Progression of regional grey matter atrophy in multiple sclerosis. *Brain*. 2018;141:1665-1677.
- Fleischer V, Ciolac D, Gonzalez-Escamilla G, et al. Subcortical volumes as early predictors of fatigue in multiple sclerosis. *Ann Neurol*. 2022;91:192-202.
- De Stefano N, Stromillo ML, Giorgio A, et al. Establishing pathological cut-offs of brain atrophy rates in multiple sclerosis. *J Neurol Neurosurg Psychiatry*. 2016;87:93-99.
- Kappos L, Wolinsky JS, Giovannoni G, et al. Contribution of relapse-independent progression vs relapse-associated worsening to overall confirmed disability accumulation in typical relapsing multiple sclerosis in a pooled analysis of 2 randomized clinical trials. *JAMA Neurol*. 2020;77:1132-1140.
- Lublin FD, Haring DA, Ganjgahi H, et al. How patients with multiple sclerosis acquire disability. *Brain*. 2022;145:3147-3161.
- Alexander-Bloch A, Giedd JN, Bullmore E. Imaging structural covariance between human brain regions. *Nat Rev Neurosci*. 2013;14:322-336.
- Chard DT, Alahmadi AAS, Audoin B, et al. Mind the gap: From neurons to networks to outcomes in multiple sclerosis. *Nat Rev Neurol*. 2021;17:173-184.
- Tijms BM, Series P, Willshaw DJ, Lawrie SM. Similarity-based extraction of individual networks from gray matter MRI scans. *Cerebral cortex*. 2012;22:1530-1541.
- Fleischer V, Radetz A, Ciolac D, et al. Graph theoretical framework of brain networks in multiple sclerosis: A review of concepts. *Neuroscience*. 2019;403:35-53.
- Zielinski BA, Gennatas ED, Zhou J, Seeley WW. Network-level structural covariance in the developing brain. *Proc Natl Acad Sci U S A*. 2010;107:18191-18196.
- Mechelli A, Friston KJ, Frackowiak RS, Price CJ. Structural covariance in the human cortex. *J Neurosci*. 2005;25:8303-8310.
- Bullmore E, Sporns O. The economy of brain network organization. *Nat Rev Neurosci*. 2012;13:336-349.
- He Y, Dagher A, Chen Z, et al. Impaired small-world efficiency in structural cortical networks in multiple sclerosis associated with white matter lesion load. *Brain*. 2009;132(12):3366-3379.
- Fleischer V, Koirala N, Drobny A, et al. Longitudinal cortical network reorganization in early relapsing-remitting multiple sclerosis. *Ther Adv Neurol Disord*. 2019;12:1756286419838673.
- Tur C, Eshaghi A, Altmann DR, et al. Structural cortical network reorganization associated with early conversion to multiple sclerosis. *Sci Rep*. 2018;8:10715.
- Koubyr I, Besson P, Deloire M, et al. Dynamic modular-level alterations of structural-functional coupling in clinically isolated syndrome. *Brain*. 2019;142:3428-3439.

22. Muthuraman M, Fleischer V, Kolber P, Luessi F, Zipp F, Groppa S. Structural brain network characteristics can differentiate CIS from early RRMS. *Front Neurosci.* 2016;10:14.
23. Tur C, Kanber B, Eshaghi A, et al. Clinical relevance of cortical network dynamics in early primary progressive MS. *Mult Scler.* 2020;26:442-456.
24. Rimkus CM, Schoonheim MM, Steenwijk MD, et al. Gray matter networks and cognitive impairment in multiple sclerosis. *Mult Scler.* 2019;25:382-391.
25. Collorone S, Prados F, Hagens MH, et al. Single-subject structural cortical networks in clinically isolated syndrome. *Mult Scler.* 2020;26:1392-1401.
26. Bevan CJ, Cree BA. Disease activity free status: A new end point for a new era in multiple sclerosis clinical research? *JAMA Neurol.* 2014;71:269-270.
27. Kalincik T, Cutter G, Spelman T, et al. Defining reliable disability outcomes in multiple sclerosis. *Brain.* 2015;138(11):3287-3298.
28. Schmidt P, Gaser C, Arsic M, et al. An automated tool for detection of FLAIR-hyperintense white-matter lesions in multiple sclerosis. *Neuroimage.* 2012;59:3774-3783.
29. Tustison NJ, Avants BB, Cook PA, et al. N4ITK: Improved N3 bias correction. *IEEE Trans Med Imaging.* 2010;29:1310-1320.
30. Ashburner J, Ridgway GR. Symmetric diffeomorphic modeling of longitudinal structural MRI. *Front Neurosci.* 2012;6:197.
31. Ashburner J. A fast diffeomorphic image registration algorithm. *Neuroimage.* 2007;38:95-113.
32. Ashburner J, Friston KJ. Unified segmentation. *Neuroimage.* 2005; 26:839-851.
33. Lorio S, Fresard S, Adaszewski S, et al. New tissue priors for improved automated classification of subcortical brain structures on MRI. *Neuroimage.* 2016;130:157-166.
34. Gonzalez-Escamilla G, Ciolac D, De Santis S, et al. Gray matter network reorganization in multiple sclerosis from 7-tesla and 3-tesla MRI data. *Ann Clin Transl Neurol.* 2020;7:543-553.
35. Gonzalez-Escamilla G, Miederer I, Grothe MJ, et al. Metabolic and amyloid PET network reorganization in Alzheimer's disease: Differential patterns and partial volume effects. *Brain Imaging Behav.* 2021;15:190-204.
36. Rubinov M, Sporns O. Complex network measures of brain connectivity: uses and interpretations. *Neuroimage.* 2010;52:1059-1069.
37. Latora V, Marchiori M. Efficient behavior of small-world networks. *Phys Rev Lett.* 2001;87:198701.
38. Newman ME, Park J. Why social networks are different from other types of networks. *Phys Rev E Stat Nonlin Soft Matter Phys.* 2003;68(3 Pt 2):036122.
39. DeLong ER, DeLong DM, Clarke-Pearson DL. Comparing the areas under two or more correlated receiver operating characteristic curves: A nonparametric approach. *Biometrics.* 1988;44:837-845.
40. Trapp BD, Peterson J, Ransohoff RM, Rudick R, Mork S, Bo L. Axonal transection in the lesions of multiple sclerosis. *N Engl J Med.* 1998;338:278-285.
41. De Stefano N, Giorgio A, Battaglini M, et al. Assessing brain atrophy rates in a large population of untreated multiple sclerosis subtypes. *Neurology.* 2010;74:1868-1876.
42. Tur C, Carbonell-Mirabent P, Cobo-Calvo A, et al. Association of early progression independent of relapse activity with long-term disability after a first demyelinating event in multiple sclerosis. *JAMA Neurol.* 2023;80:151-160.
43. Schoonheim MM, Broeders TAA, Geurts JGG. The network collapse in multiple sclerosis: an overview of novel concepts to address disease dynamics. *Neuroimage Clin.* 2022;35: 103108.
44. Popescu V, Klaver R, Voorn P, et al. What drives MRI-measured cortical atrophy in multiple sclerosis? *Mult Scler.* 2015;21: 1280-1290.
45. van Olst L, Rodriguez-Mogeda C, Picon C, et al. Meningeal inflammation in multiple sclerosis induces phenotypic changes in cortical microglia that differentially associate with neurodegeneration. *Acta Neuropathol.* 2021;141:881-899.
46. Kiljan S, Meijer KA, Steenwijk MD, et al. Structural network topology relates to tissue properties in multiple sclerosis. *J Neurol.* 2019;266:212-222.
47. Fleischer V, Groger A, Koirala N, et al. Increased structural white and grey matter network connectivity compensates for functional decline in early multiple sclerosis. *Mult Scler.* 2017;23: 432-441.
48. Brownlee WJ, Altmann DR, Prados F, et al. Early imaging predictors of long-term outcomes in relapse-onset multiple sclerosis. *Brain.* 2019;142:2276-2287.
49. Giorgio A, Stromillo ML, De Leucio A, et al. Appraisal of brain connectivity in radiologically isolated syndrome by modeling imaging measures. *J Neurosci.* 2015;35:550-558.
50. Gong G, He Y, Chen ZJ, Evans AC. Convergence and divergence of thickness correlations with diffusion connections across the human cerebral cortex. *Neuroimage.* 2012;59: 1239-1248.
51. Alexander-Bloch A, Raznahan A, Bullmore E, Giedd J. The convergence of maturational change and structural covariance in human cortical networks. *J Neurosci.* 2013;33:2889-2899.
52. Khundrakpam BS, Lewis JD, Jeon S, et al. Exploring individual brain variability during development based on patterns of maturational coupling of cortical thickness: A longitudinal MRI study. *Cerebral cortex.* 2019;29:178-188.
53. Rocca MA, Valsasina P, Meani A, et al. Network damage predicts clinical worsening in multiple sclerosis: A 6.4-year study. *Neurol Neuroimmunol Neuroinflamm.* 2021;8:e1006.